UCRL- 95144
PREPRINT

Hard-Sphere Heat Conductivity via Nonequilibrium Molecular Dynamics

Karl W. Kratky
William G. Hoover

This paper was prepared for submittal to
Journal of Statistical Physics

August 12, 1986

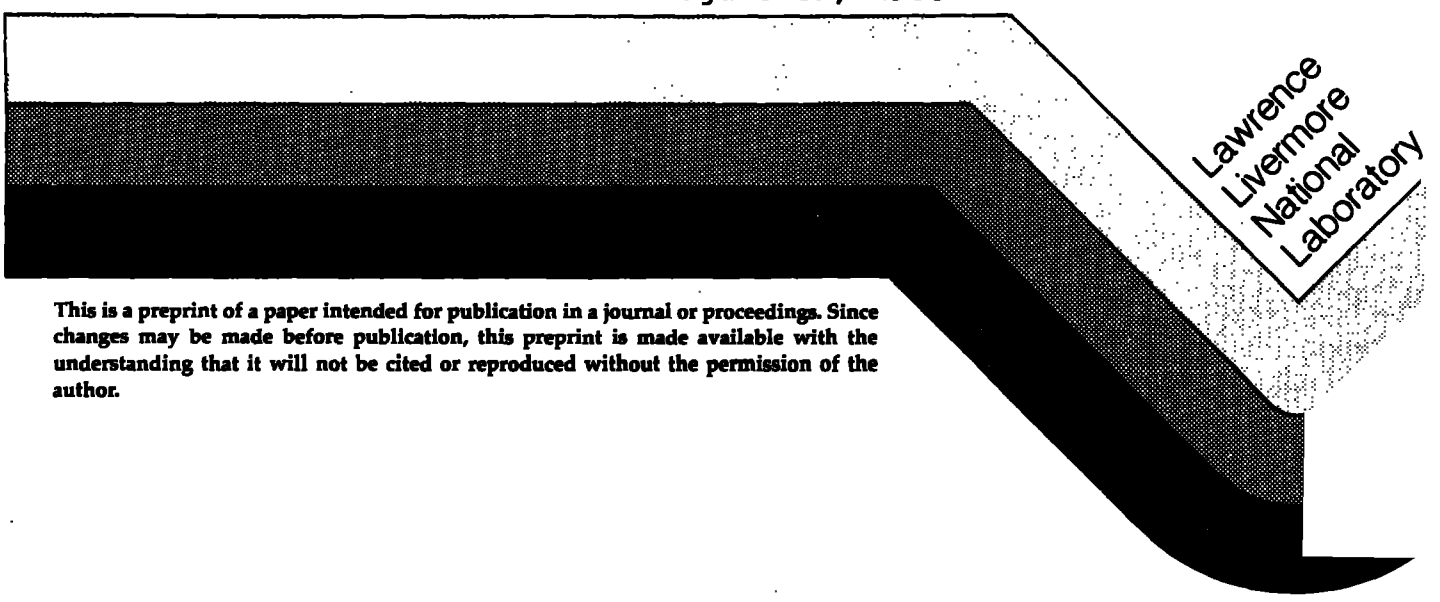

DISCLAIMER

HARD-SPHERE HEAT CONDUCTIVITY VIA NONEQUILIBRIUM MOLECULAR DYNAMICS

Karl W. Kratky
Institut für Experimentalphysik, Universität Wien
Boltzmanngasse 5, A-1090 Wien, Austria

William G. Hoover
Department of Applied Science
University of California at Davis
and Lawrence Livermore National Laboratory
Post Office Box 808
Livermore, California 94550, United States of America

ABSTRACT:

We use an Evans-Gillan driving force F_d, together with isokinetic and isoenergetic constraint forces F_c, to drive steady heat currents in periodic systems of 4 and 32 hard spheres. The additional driving and constraint forces produce curved trajectories as well as additional streaming and collisional contributions to the momentum and energy fluxes. Here we develop an analytic treatment of the collisions approximately 10 times faster than our previous numerical treatment. At low field strengths λ, for $\lambda\sigma$ less than 0.4, where σ is is the hard-sphere diameter, the 32-sphere conductivity is consistent with Alder, Gass and Wainwright's 108-sphere value. At higher field strengths the conductivity varies roughly as $\lambda^{1/2}$, in parallel to the logarithmic dependence found previously for 3 hard disks.

Key words: Nonequilibrium molecular dynamics, heat conductivity, hard spheres

I. INTRODUCTION

Boltzmann formulated the atomistic basis for nonequilbirium flows of mass, momentum, and energy, described by the linear laws of Fick, Newton, and Fourier [1]. A general method for expressing the corresponding transport coefficients, the diffusion, viscosity, and heat conductivity, in terms of equilibrium current, stress, and heat current autocorrelation time integrals was developed by Green and Kubo. Alder and Wainwright applied this linear response formalism to the simplest prototypical atomic model, hard spheres, during the period from 1955 to 1970 [2,3].

A major accomplishment of the computational effort during this period was establishing the form of equilibrium equation of state, characterizing the number-dependence of the pressure [2,4] and establishing the location of the fluid-solid phase transition [5]. This work led to a fairly reliable method for calculating fluid-phase equilibrium properties by perturbation theory based on the hard-sphere results [6]. Nonequilibrium progress has been more difficult, primarily due to the lack of a useful perturbation theory. The Green-Kubo method provided a route to the linear transport coefficients using equilibrium molecular dynamics. Because the calculations were time-consuming, being based on the analysis of fluctuations, and showed considerable number dependence, there was motivation to develop alternative approaches [7,8].

New methods began to be developed for treating nonlinear transport, using driving forces and constraint forces to produce fluxes under steady-state, far-from-equilibrium conditions. By 1982 Evans and Gillan had shown that heat flow, the transport property studied here, could be induced by using a driving force depending on individual particle contributions to the energy and pressure tensor [9,10]. Their idea has been applied to both soft [11,12] and hard [13] spheres. Heat flow requires a system of three or more particles and is intrinsically more complex than diffusive or viscous flows, for which two particles suffice [14]. Here we apply the Evans-Gillan idea to hard spheres.

The present work is organized as follows. In Section II we give a brief resume of the Evans-Gillan recipe for the determination of the heat conductivity. In Section III we describe an analytic method which makes the collisional calculation more efficient than the purely numerical approach followed previously [13], particularly for dense fluids and for solids. Conductivity results based on this analytic approach are listed in Section IV. Section V is a discussion.

II. BASIC EQUATIONS

In the interest of generality and clarity, we first consider a continuous pairwise-additive interaction potential $\phi(r)$. We consider later the hard-sphere limit. The periodic system, which can be fluid or solid, with volume V, contains N D-dimensional particles of mass m. The total momentum

of the system is zero. Particle i, located at r_i has momentum p_i. The total energy E is a sum of kinetic and potential contributions K and Φ:

$$E = K + \Phi = \sum p_i^2/2(m) + \sum \sum \phi_{ij}(r_{ij}) \; ; \tag{1}$$

The single sum runs over all N particles. The double sum includes all pairs of particles. Three types of forces act on each particle: An <u>applied</u> force F_a from the potential gradient, an external <u>driving</u> force F_d inducing, on the average, a heat flow in the x direction, and a <u>constraint</u> force F_c fixing either the total energy E or the kinetic energy K:

$$\dot{p} = dp/dt = F_a + F_c + F_d, \; 1 \leq i \leq N \; ;$$

$$r_{ij} \equiv r_i - r_j \; ,$$

$$F_i \equiv \sum_j F_{ij} \tag{2}$$

$$F_d \equiv \lambda(\Delta E + V\Delta P^{\phi}_{xx}, \; V\Delta P^{\phi}_{xy}, \; V\Delta P^{\phi}_{xz})$$

$$F_c \equiv - \zeta_E p \text{ or } - \zeta_K p \; .$$

$\Delta E = \Delta E_i$ indicates the actual instantaneous energy for particle i minus the average energy per particle, E/N, at the same time:

$$\Delta E_i = [\, p_i^2/(2m) + \tfrac{1}{2} \sum \phi_{ij}] - [E/N] \; . \tag{3}$$

The sum runs over all particles j interacting with i. Similarly, the individual-particle fluctuations in potential pressure-tensor components,

$$\Delta P^{\phi}_{x\alpha,i} = P^{\phi}_{x\alpha,i} - P^{\phi}_{x\alpha} \; . \tag{4}$$

follow from the definition of the instantaneous pressure tensor:

$$P_{\alpha\beta}V = P^{K}_{\alpha\beta}V + P^{\Phi}_{\alpha\beta}V = \Sigma\, p_\alpha p_\beta/m + \Sigma\,\Sigma\, r_\alpha F_\beta \ ; \tag{5}$$

Note that only the potential part P^{Φ} of the pressure tensor contributes to the driving force F_d. This force is constructed so as to induce a mean heat flux in the x-direction with the resulting dissipation matching that from irreversible thermodynamics [9]. The instantaneous heat flux Q is given by

$$mQV = \Sigma\, p_i E_i + \Sigma\,\Sigma\, r_{ij}\,[\,\tfrac{1}{2}(p_i + p_j)\cdot F_{ij}] \ . \tag{6}$$

Because the total momentum vanishes Q is identically zero in a two-body system. In the constraint force F_c, the friction coefficient ζ_E or ζ_K is a function of time, but has the same value for all particles. ζ is chosen so that either the total energy E or the kinetic part K is a constant of motion. The two choices will be called "isoenergetic" and "isokinetic", respectively. Explicit construction of ζ yields [11]

$$\begin{aligned} \zeta_E &= \lambda Q_x V/(2K) \ , \\ \zeta_K &= \zeta_E + [\Sigma\, p_i \cdot F_i/(2Km)] \end{aligned} \tag{7}$$

for the isoenergetic and isokinetic cases, respectively. One can see that for absent driving force (λ=0), ζ_E is also vanishing. This corresponds to the usual Newtonian equilibrium molecular dynamics. In ζ_K, however, there is an extra term independent of λ. Thus, even for λ=0, the isokinetic molecular dynamics is non-Newtonian [13].

Measuring the heat flux Q makes it possible to obtain the thermal conductivity κ from the relation [11]

$$\bar{Q}_x = \kappa\lambda T \ . \tag{8}$$

The bar means time average. T is the absolute temperature defined by the relation

$$\bar{K} = \frac{1}{2} DNkT \ , \tag{9}$$

where k is Boltzmann's constant.

Equation (8) may be used for <u>any</u> λ to define formally a nonequilibrium $\kappa = \kappa(\lambda)$. To compare with linear Green-Kubo results [3], however, small λ's have to be used. Equation (8) may be compared with Fourier's Law:

$$Q = - \kappa \nabla T \tag{10}$$

which likewise defines a constant κ (linear regime) only for small temperature gradients.

Both Q_x and κ depend on N. One might conjecture that κ is a monotonically increasing function of N up to the thermodynamic limit. The form of this number dependence was discussed, qualitatively, in Reference [3].

The meaning of <u>temperature</u> for small systems was discussed in Reference [15]. We use temperature in the sense of $\tilde{T}$ of that reference, generalized to nonequilibrium systems. Furthermore, the thermodynamic <u>pressure</u> in D dimension given by the usual relation

$$P = \sum_{\alpha} \bar{P}_{\alpha\alpha}/D \ . \tag{11}$$

III. CALCULATION METHOD

A. Streaming Motion ($\Phi = 0$)

We consider an interaction potential which vanishes for $r>\sigma$, so that we have soft repulsive spherical particles of diameter σ. If no pair of particles overlaps, then $\phi=0$, and the isoenergetic and isokinetic cases coincide. The corresponding "streaming motion" is characterized by

$$dp_{\alpha i}/dt = \lambda\delta_{\alpha x}(\Delta K) - \zeta p_{\alpha i} ,$$
$$\zeta = \lambda \sum p_{xi}\Delta K_i/(2Km) . \qquad (12)$$

K and ΔK appear, rather than the ΔE of (2) because the potential vanishes between collisions. The ND equations of motion are coupled by ζ. Equations (5) and (6) are simplified:

$$P_{\alpha\beta}V = \sum p_{\alpha i}p_{\beta i}/m , \qquad (13)$$

$$mQV = \sum p_i K_i = \sum p_i \Delta K_i , \qquad (14)$$

for the streaming motion. Combination of (9), (11) and (13) shows that $PV/(NkT)=1$ as in the equilibrium case.

Setting $\sigma=0$ yields the ideal gas case. Then <u>only</u> streaming motion occurs, which is in general no longer characterized by straight lines if $\lambda\neq 0$. Without loss of generality, we assume $\lambda\geq 0$ in the following. What is the maximum Q_x which can be achieved for given N,D and kT when the center of

mass is fixed? A Lagrange-multiplier calculation yields the result that one particle (say particle 1) moves in the positive x-direction. The rest move in the opposite direction:

$$p_i = -p_1/(N-1) \ , \ 2 \le i \le N \ ;$$
$$K = \frac{1}{2} DNkT = p_1^2/[m(1-N^{-1})] \ . \tag{15}$$

The corresponding heat flux is

$$mQ_x^{max}V = \frac{1}{2}(1-2N^{-1})\,[m(DNkT)^3/(1-N^{-1})]^{1/2} \ . \tag{16}$$

Thus the collisionless ideal-gas behavior may be characterized as follows: For small λ, Q_x increases proportional to λ, as given by (8). If λ becomes very large, or, if the streaming motion persists for a long time, Q_x tends to a saturation value Q^{max} given in (16). Accordingly, κ becomes proportional to $1/\lambda$ for large λ. Between collisions, the streaming motion is the same as that of an ideal gas and can be treated numerically without problems. The streaming motion ends when any pair of particles happens to touch. Without loss of generality, we assume a collision of particles 1 and 2 in the following.

B. Collisions

In our preliminary calculations in reference [13], the colliding motion was treated numerically assuming potentials proportional to $\sigma - r$ for $\sigma > r$ and vanishing for $\sigma < r$. The equations of motion were solved for a series of increasing proportionality constants until the "hard-sphere limit" was

achieved. Because ϕ was continuous the motion, pressure, and heat flux vector could all be calculated without trouble. The pressure and heat flux contributions from the collisions are not the same for isoenergetic and isokinetic cases. This comes from the different momentum histories during the collision. Of course at the end of collision (defined by $r_{12} = \sigma$) the motions coincide in the two cases. This is because the extra net work performed by the driving force during each collision is exactly offset by the isoenergetic or isokinetic friction coefficient. Thus the coordinate trajectories are the same in the hard-sphere limit. The numerical calculation of collisions was relatively slow because the momenta of all the particles varied with time. In the present paper, we display a theoretical treatment of collisions which substantially reduces this numerical work. Only two-particle collisions 1-2 have to be considered. During each collision, the product of force and distance greatly exceeds kT, and the distance vector r_{12} is essentially constant, equal to σ. In this limit Eq. (2) becomes

$$\dot{p}_i = dp_i/dt = N_i F_{12} e_{12} - \zeta p_i \ , \ 1 \le i \le N \quad , \tag{17}$$

where e_{12} is a unit vector parallel to r_{12}, and with F_{12} the magnitude of the force exerted on particle 1 by particle 2.

$$\begin{aligned} N_1 &\equiv 1 + \tfrac{1}{2}\lambda x_{12}(1-2N^{-1}) \ , \\ N_2 &\equiv -1 + \tfrac{1}{2}\lambda x_{12}(1-2N^{-1}) \ , \\ N_i &\equiv -\lambda x_{12}/N \ , \quad 3 \le i \le N \ . \end{aligned} \tag{18}$$

The terms linear in λ come from the driving force. The general solution of (17) is

$$p_i(t) = [I(t)]^{-1} \left[p_i(o) + e_{12}N_i \int_o^t F_{12}(t')I(t')dt'\right] ,$$
$$I(t) = \exp \int_o^t \zeta(t')dt' , \tag{19}$$

with o indicating the time at the beginning of collision. This solution, however, can only be used if ζ is known as a function of t. The friction coefficients which couple the ND differential equations are given by (7) as follows:

$$\zeta_E = F_{12} \ \tfrac{1}{2}[\lambda x_{12}(p_1+p_2)]/(2Km) , \tag{20}$$

$$\zeta_K = F_{12} \ \tfrac{1}{2}[\lambda x_{12}(p_1+p_2) + (p_1-p_2)]/(2Km) , \tag{21}$$

It is convenient to use the notation $p_{12} \equiv p_1-p_2$ and $s_{12} \equiv p_1+p_2$ for the relative and total momenta of the colliding pair. Then (18) yields

$$\dot{p}_{12} = 2F_{12} - \zeta\, p_{12} , \tag{22}$$

$$\dot{s}_{12} = \lambda x_{12}(1-2N^{-1}) \ F_{12} - \zeta\, s_{12} . \tag{23}$$

Projection onto $e_{12} = r_{12}/\sigma$, indicated by a prime, gives

$$\dot{p}'_{12} = 2F_{12} - \zeta p'_{12} , \tag{24}$$

$$\dot{s}'_{12} = [\lambda x_{12}(1-2N^{-1})]\, F_{12} - \zeta\, s'_{12} , \tag{25}$$

where F_{12} is a steep repulsive force yet to be chosen explicitly.

The isoenergetic case is characterized by

$$\zeta_E = F_{12}[\tfrac{1}{2}\lambda x_{12}s'_{12}]/(2Km) ,$$
$$(\dot{E}=0) \rightarrow (\dot{K} = -\dot{\Phi} = F_{12}p'_{12}/m) . \tag{26}$$

The isokinetic case is given by

$$\zeta_K = F_{12}\,[\tfrac{1}{2}\lambda x_{12}s'_{12} + p'_{12}]/(2Km)\ , \qquad (27)$$

$$(\mathring{K}=0) \rightarrow (K=\text{constant})\ .$$

Thus, the isoenergetic case has been reduced to three coupled differential equations in the variables p'_{12}, s'_{12} and K. The isokinetic case has been reduced to two coupled equations in the variable p'_{12} and s'_{12}. Because this is simpler, the isokinetic case will be solved first.

Having the solution for p'_{12}, s'_{12}, K means first knowing ζ. See (26) and (27). Then the momenta $p_{\leftarrow i}$ during the collision follow from (19).

Furthermore, the instantaneous pressure and heat flux follow from (5) and (6):

$$p_{\alpha\beta}V = F_{12}\sigma e_{\alpha,12}e_{\beta,12}\ , \qquad (28)$$

$$mQ_\alpha V = \tfrac{1}{2}F_{12}\sigma e_{\alpha,12}s'_{12}\ . \qquad (29)$$

Generally each collision begins with $p'_{12}<0$ and ends with $p'_{12}>0$. The turning point is given by $p'_{12}=0$. The condition ending the collision, $\int p'_{12}dt=0$, is discussed below.

C. Isokinetic Hard-Sphere Collisions

The colliding motion begins at time 0 and ends at time t_c with $r_{12}=\sigma$. We assume that the force during the penetration of the spheres is

$$F_{12} = F\,e_{12} \qquad (30)$$

with arbitrarily high, but finite, F. Then, (24), (25) and (27) may be combined to give a single differential equation for ζ_K:

$$\dot{\zeta}_K = F^2[(1 + \tfrac{1}{2}\delta)/(mK)] - \zeta_K^2 ,$$
$$\delta \equiv \tfrac{1}{2}(1-2N^{-1})\lambda^2 x_{12}^2 \geq 0 . \tag{31}$$

For the duration of each collision δ is fixed, and gives the influence of the driving force F_1^d on the collision. It is convenient to replace the time variables ζ and t by impulse variables X_K and τ:

$$X_K = \zeta_K/F , \quad \tau = Ft . \tag{32}$$

During the collision, $0 < \tau < \tau_c$. In the hard-sphere limit, as the collision time t_c tends to zero the absolute value of ζ_K becomes arbitrary large, but the impulse delivered remains finite and non-vanishing. We will see that similar considerations hold for pressure and heat flux. Using the definitions (32), Equation (31) becomes

$$dX_K/d\tau = (d\zeta_K/dt)/F^2 = q^2 - X_K^2$$
$$q \equiv [(1 + \tfrac{1}{2}\delta)/(mK)]^{1/2} \tag{33}$$

From the definition of q and X_K it follows that

$$q^2 - X_K^2 \geq 0 \tag{34}$$

during the whole collision.

The solution of (33) is

$$X_K = q\,[1 - 2/(1+\Omega\exp(2q\tau)],$$
$$\Omega = [q+X_K(o)][q-X_K(o)] , \quad 0 < \Omega < X \tag{35}$$

X increases monotonically with time. Because we know the friction, equations (17) can be solved separately. The result is

$$p_i(\tau) = [I(\tau)]^{-1} \left[p_i(o) + e_{12}N_i \int_o^\tau I(\tau')d\tau'\right] ,$$

$$I(\tau) = [\Omega\exp(q\tau) + \exp(-q\tau)]/(1+\Omega) , \tag{36}$$

$$\int_o^\tau I(\tau')d\tau' = [1-\Omega+\Omega\exp(q\tau)-\exp(-q\tau)[/q(1+\Omega)] .$$

Now it has to be determined when the collision ends. The condition corresponding to a net displacement of zero, the hard-sphere limit, is

$$\int_o^{\tau_c} p'_{12}(\tau)\, d\tau = Fm[r'_{12}(\tau_c) - \sigma] = 0. \tag{37}$$

From (36), this can be written as

$$\ln I(\tau_c) = - d_a \tan^{-1} d_b(\tau_c) ,$$

$$d_a = [1 - \Omega + \tfrac{1}{2}(1+\Omega)\, q\, p'_{12}]/\Omega^{1/2} , \tag{38}$$

$$d_b(\tau_c) = \Omega^{1/2} [\exp(q\tau_c) - 1]/[1+\Omega\exp(q\tau_c)] .$$

As usual, $p'_{12}=p'_{12}(\tau=0)$. The trivial solution of (38) with $\tau=0$ and $r'_{12}=\sigma$ corresponds to the <u>beginning</u> of the collision. There is a second unique solution with $0 < \tau_c < \infty$ and $r_{12}=\sigma$ determining the <u>end</u> of the collision. This solution has to be found numerically. Then, the pressure (28) and heat flux (29) integrals yield

$$\int_{coll} p_{\alpha\beta} V dt = \sigma\, e_{\alpha,12} e_{\beta,12}\, \tau_c \quad , \tag{39}$$

$$\int_{coll} mQ_\alpha V dt = \tfrac{1}{2}\sigma\, e_{\alpha,12} \int_{coll} s'_{12}(\tau)\, d\tau =$$

$$= \tfrac{1}{2}\sigma e_{\alpha,12} [(1+\Omega)/(mq\Omega^{1/2})] [s'_{12} - \tfrac{1}{2}\lambda x_{12}(1-2N^{-1})p'_{12}] \tan^{-1} d_b(\tau_c) , \tag{40}$$

Combination of (27), (29) and (37) results in

$$\int \zeta_K dt = \int X_K d\tau = [\lambda/(2Km)] \int mQ_x V dt \ .$$

where the integrals cover the ranges $0 < t < t_c$ and $0 < \tau < \tau_c$. For $d_b(\tau_c)$, see (38). Thus, the complete solution for $X_K > -q$ has been found. If X_K is equal to $-q$, a limiting case of zero probability, both th collision time t_c and the impulse delivered τ_c diverge.

D. Isoenergetic Hard-Sphere Collisions

The three coupled equations for the isoenergetic case are

$$\dot{p}'_{12} = F_{12} [2 - \lambda x_{12} s'_{12} p'_{12}/(4Km)] \ , \tag{41}$$

$$\dot{s}'_{12} = F_{12} \lambda x_{12} [(1-2N^{-1}) - [(s'_{12})^2/(4Km)]], \tag{42}$$

$$\dot{Km} = F_{12} p'_{12} \ . \tag{43}$$

The corresponding values of ζ_E, $P_{\alpha\beta}$ and Q_α are given by (26), (28) and (29), respectively.

We introduce the new variables u,v,w

$$u \equiv \frac{1}{2} \lambda x_{12} s'_{12} \ , \ v = \frac{1}{2} \delta p'_{12} \ , \ w = 2\delta Km \ . \tag{44}$$

into (41) to (43) and find

$$\dot{u} = \delta F_{12} [1-(u^2/w)], \tag{45}$$

$$\dot{v} = \delta F_{12}[1-(uv/w)] , \tag{46}$$

$$\dot{w} = \delta F_{12}[4v/\delta] . \tag{47}$$

$F_{12} >> 0$ is not yet specified. In the above variables,

$$\delta_E = \delta F_{12} u/w ; \tag{48}$$

see (26).

Assuming that F_{12} is constant is not useful here, but a more complicated assumption, which gives a constant friction coefficient ζ_E, <u>does</u> make the system tractable:

$$F_{12} = Cw \, sgn(u)/(u\delta) . \tag{49}$$

Thus F_{12} varies during the collision. Because δ is infinitesimal while $w>0$, $F_{12}\sigma/kT>>0$. Thus $F\to\infty$ yields again the hard-sphere limit. If u changes sign during the collision, F_{12} would approach ∞ at this point even for finite F. We will see later that this causes no difficulty. The friction coefficient becomes

$$\zeta_E = C \, sgn(u) . \tag{50}$$

Defining $\tau=Ct$ as usual, (45) to (47) become

$$du/d\tau = sgn(u) [w-u^2]/u , \tag{51}$$

$$dv/d\tau = sgn(u) [w-uv]/u , \tag{52}$$

$$dw/d\tau = sgn(u) [4wv]/(\delta u) . \tag{53}$$

Subtracting (51) from (52) yields

$$d(v-u)/d\tau = -sgn(u) [v-u] . \tag{54}$$

This can be solved, with the result:

$$v(\tau) - u(\tau) = (v-u)\, ex(\tau) ,$$

$$ex(\tau) \equiv \begin{cases} \exp(-\tau) & : \ u(o) \geq 0 \\ \exp(\tau) & : \ 0 \geq u \\ \exp(2\tau^* - \tau) & : \ u > 0 > u(o) . \end{cases} \tag{55}$$

From the definitions of u and w it follows that $w > u^2$ in the present case. Therefore, $du/d\tau > 0$ during the collision. Thus, $u > u(o)$ for $\tau > 0$. τ^* is defined by $u(\tau^*) = 0$, i.e., when u changes sign (which need not happen). Since determines the time behavior of (v-u), we make the assumption

$$u(\tau) \equiv g(\tau)\, ex(\tau) . \tag{56}$$

defining a function $g(\tau)$. It follows that

$$g(o) = u(o),\ sgn(g) = sgn(u),\ du/d\tau = [(dg/d\tau) - sgn(g)\ g]\ ex(\tau). \tag{57}$$

Inserting (55) yields

$$v = (g + v - u)\, ex(\tau) . \tag{58}$$

On the other hand, from (51) it follows that

$$w = sgn(g)\ g\ (dg/d\tau)\ ex^2(\tau). \tag{59}$$

Thus we have expressed u,v and w in terms of a single unknown function g. $(du/d\tau) > 0$ means $(dg/d\tau) > 0$; see (57). Thus g is strictly increasing with τ. $g(\tau^*) = 0$ defines τ^*. Generally, w is non-negative due to (59). Because w is proportional to $K > 0$, w cannot vanish, even for $g \to 0$. This means that at $\tau \to \tau^*$, $|g|(dg/d\tau)$ remains finite and nonzero. That $(dg/d\tau) \to \infty$ when $\tau \to \tau^*$, we can see from (51).

Utilizing (53) yields the desired differential equation for g:

$$[g(d^2g/d\tau^2) - (dg/d\tau)^2]\delta sgn(g) = 2(dg/d\tau)[g(\delta+2)+2(v(o)-u(o)] \ . \quad (60)$$

Using the transformation $p \equiv dg/d\tau$ one can solve the resulting first-order differential equation in p (as function of g). Reinserting $p=dg/d\tau$ yields

$$gdg/(ag^2 + bg + c) = sgn(g)\ d\ \tau \ ,$$
$$a \equiv 1 + (2/\delta),\ b \equiv (4/\delta)\ (v-u)\ ,\ c \equiv w - au^2 - bu \ . \quad (61)$$

The donominator is nonvanishing for any g if

$$\Delta \equiv 4ac - b^2 = 4[1+(2/\delta)w] - 4[u+(2/\delta)v]^2 > 0. \quad (62)$$

From the definition of u, v and w it follows that $\Delta \geq 0$ generally if $\delta>0$. The zero-probability case $\Delta=0$ occurs if and only if u=v and w=u [1+(2/δ)] corresponding to the vanishing of the kinetic energy at the turning point. Thus Δ is positive and equation (61) can be solved for τ as a function of g:

$$ex(\tau) = \left(\frac{ag^2+bg+c}{ag^2+bg+c}\right)^{1/(2a)} \exp\ \frac{b}{a\Delta^{1/2}} \tan^{-1}\ \frac{\Delta^{1/2}(g-g)}{2agg+b(g+g)+2c} \ . \quad (63)$$

Combining (59) and (61) yields the simple relations

$$w = (ag^2+bg+c)\ ex^2(\tau)\ ,\ w = ag^2+bg+c \ . \quad (64)$$

The end of collision is given by $w_{end} = w$, cf. (6.26). Thus,

$$ex(\tau_c) = [w(o)/(ag_c^2 + bg_c + c)]^{1/2} \ . \quad (65)$$

Inserting this result in (63) yields an equation for g_c:

$$(1-a)\Delta^{1/2}\,\ell n\,[(ag_c^2+bg_c+c)/\delta] = 2b\,\tan^{-1}\,\frac{\Delta^{1/2}(g_c-g)}{2ag_cg+b(g_c+g)+2c}\quad . \tag{66}$$

This equation has a unique solution for $g_c>g$, which has to be determined numerically. This may be compared with the general isokinetic case, where a formally similar but simpler equation, (38), gave τ_c.

We may evaluate τ_c using (65) and the solution of (66). It is possible, however, to express all quantities in terms of g_c. For u,v,w see Eqs. (56), (58) and (64), respectively, inserting (65) for $ex(\tau)$. Bearing in mind that $\zeta_E=C\,sgn(u)$, the momenta at the end of collision are

$$p_i(g_c) = ex(\tau(g_c))\,[p_i + e_{12}N_i(g_c-g)/\delta]\quad . \tag{67}$$

Furthermore, the collisional integral of the friction coefficient is given by

$$\int \zeta_E\,dt = -\,\ell n\,ex(\tau_c) = \frac{1}{2}\,\ell n\,[(ag_c^2+bg_c+c)/w]\quad . \tag{68}$$

The corresponding pressure and heat flux contributions are evaluated easily numerically:

$$\int p\,V_{a\beta}dt = \delta\,e_{\alpha,12}e_{\beta,12}\delta^{-1}\int_g^{g_c} ex(\tau(g))dg\quad , \tag{69}$$

$$\int mQ_\alpha V\,dt = \frac{1}{2}\,\delta\,e_{\alpha,12}(\delta\lambda x_{12})^{-1}\int_g^{g_c} ex^2(\tau(g))gdg\quad , \tag{70}$$

which completes the solution.

IV. COMPUTER EXPERIMENTAL RESULTS

In Section III, the collisions were reduced to one-dimensional quadratures. The solutions were built into the existing computer program [13] which can treat two- , three- and four-dimensional systems. A series of test runs showed that the reduction in computer time used varies with the number of particles, dimensionality, and density, but is typically a factor 10. For very low densities, where streaming motion is dominant, the gain is only about a factor of two.

In this paper, results for hard spheres are presented. The following particle numbers and densities were investigated:

$(N=4, V/V_0 = 1.25)$ & $(N=32, V/V_0=1.25)$: typical solid,

$(N=4, V/V_0 = 1.80)$ & $(N=32, V/V_0=1.80)$: dense fluid,

$(N=4, V/V_0 = 3.00)$: dilute fluid.

V_0 is the close-packed volume $N\sigma^3/\sqrt{2}$. For each of the five series of computer experiments, $\lambda^{1/2}$ was varied between 0.0 and 2.0 in steps of 0.1. Details can be found in Table I. The quantities calculated are displayed in Table II. Apart from the heat flux data, the results for t^{str}, Z_E and $(Z_K-1)/(Z_E-1)$ are also presented in Tables III to VII. t^{str} is the average time between collisions and Z is the compressibility factor PV/(NkT). For $\lambda=0$ (i.e., equilibrium), it is possible to compare t^{str} and Z_E with values given in Ref. [2], where the same particle numbers and densities occur. The check of consistency is successful. For equilibrium hard spheres,

$$Z_E = 1 + \pi^{1/2}/(3N\, t^{str} a_N) \;;$$

$$a_N \equiv (1-N^{-1})(\tfrac{3}{2}N)^{1/2}\, \Gamma(\tfrac{3}{2}[N-1])/\Gamma(\tfrac{3}{2}N-1) \;, \qquad (71)$$

$$a_4 = 0.8904 \;,\; a_{32} = 0.9869 \;.$$

$\Gamma(m)$ is the usual Γ-function, $(m-1)!$ for positive integral values of m. In Ref. [2], a_N - called R there - was determined experimentally. The theoretical explanation for this correction was given in Ref. [4]. Thus, there is a further check of consistency: One has to compare Z_E calculated directly from the pressure tensor with Z_E calculated indirectly from calculated via t^{str}. For small λ, the agreement is perfect. For higher λ (starting at about $\lambda^{1/2}$=0.7), the deviations become pronounced, indicating nonlinear non-equilibrium behavior.

If we look on Tables III to VII and compare t^{str} and Z_E separately for different λ's, we see analogous behavior: up to about $\lambda^{1/2}$=0.6, t^{str} and Z_E do not depend significantly on λ. For higher λ, there are systematic positive and negative deviations which are not easy to explain theoretically.

The ratio $(Z_K-1)/(Z_E-1)$ has been included for the following reason. It can be shown that for λ=0 this quantity is

$$(Z_K-1)/(Z_E-1) = \quad 1 - [D(N-1)]^{-1} \quad , \; D \geq 1, \; N \geq 2 \;, \qquad (72)$$

for N D-dimensional hard spheres, <u>independent of density</u>. The three-dimensional values for N=4 and N=32 are 1.125 and 1.011, respectively. Tables III to VII confirm this result for small λ's.

For D=1 and N=2, $(Z_K-1)/(Z_E-1)$ becomes infinite. On the other hand, $(Z_K-1)/(Z_E-1)$ converges to 1 in the thermodynamic limit. This is one feature of a general observation: The isoenergetic and isokinetic cases both converge to the same thermodynamic limit. This can easily be seen by the following argument: the "typical" potential energy ϕ_{12} during the collision (in the case of very steep soft potentials) is essentially kT, independent of N. Thus the relative contribution of ϕ_{12} to the total energy E becomes smaller as N increases:

$$E = DNkT/2, \tag{73}$$

The restrictions of constant <u>total</u> energy and constant <u>kinetic</u> energy become identical if $N\to\infty$.

Now we turn to the heat flux. Because $Q_{x,E}$ becomes proportional to λ for small λ, while its fluctuations do not diminish, the statistical accuracy of this quantity becomes poor. This is why we chose to examine more collisions for small λ, as shown in Table I. For $\lambda^{1/2} = 0.1$, however, the heat flux data were meaningless, with estimated errors as large as the mean value itself. From heat flux, the corresponding heat conductivities can be calculated using (8). κ_E and its streaming part κ^{str} are included in Tables III to VII. These quantities are highly correlated. Again, no significant dependency on λ can be detected up to $\lambda^{1/2}=0.6$. Thus one can conclude that linear heat transport is approximately valid in this region. We have used the weighted mean of the

results for $0.2 \leq \lambda^{1/2} \leq 0.6$ as estimates for the equilibrium linear heat conductivity. Table III shows these results together with the weighted means of t^{str} and Z_E for $0.0 \leq \lambda^{1/2} \leq 0.6$. As expected, κ_E for N=4 is smaller than for N=32. A comparison with Ref. [3] is also possible, where κ_E was calculated using the Green-Kubo equilibrium autocorrelation approach:

$$\begin{aligned} V/V_0 = 1.8,\ N=108 \ &: \ \kappa_E/k = 6.94 \pm 0.14 \ , \\ V/V_0 = 3.0,\ N=108 \ &: \ \kappa_E/k = 1.92 \pm 0.02 \ . \end{aligned} \tag{74}$$

One can see that for $V/V_0 = 1.8$ the result of Ref [3] and κ_E (Table III, N=32) are consistent. Thus, the N dependence is small for N greater than 32.

Finally, consider the heat conductivity for λ greater than 0.6. After a transient region, κ_E and κ^{str} become approximately linearly decreasing functions of $\lambda^{1/2}$. This behavior may be compared with Ref [13], where a system of three hard disks was investigated. There, it turned out that κ_E and κ^{str} varied linearly with $\ln\lambda$. In that case no transient region or "linear regime" could be detected. Obviously, the λ's where these transitions occur are too small to observe in two dimensions, at least with the accuracy obtained in Ref. [13]. The three-dimensional case is more favorable. It is indeed possible to get heat conductivities for hard spheres using our method in a reasonable amount of computer time.

V. CONCLUSION

The pressures found, in both the fluid and solid phases, agree nicely with those of Alder and Wainwright for field strengths below $0.4/\sigma$. In this region there is negligible coupling, less than 1%, between the heat flux and the pressure tensor.

For the conductivity we find, as predicted by Alder, Wainwright, and Gass, considerable number dependence, roughly a factor of 3 or 4, between the 4-sphere results and the 32-sphere results. The fluid data suggest a conductivity lying somewhat below the Green-Kubo value found for 108 and 500 particles in a dense fluid.

This considerable number dependence suggests that simple few-particle models based on the dense-fluid cell-model picture will not be particularly useful for thermal conductivity. This is a little surprising in view of the great success of an Einstein-like model for conductivity in generating a good corresponding-states account of conductivities for a wide range of force laws over the entire span of dense fluid conditions [16].

The uncertainty in the old Green-Kubo results was 2% after 20,000 collisions per particle. Our uncertainty, 5% for field strengths greater than $0.05/\sigma$, based on about 1500 collisions per particle, is only a relatively small improvement over the estimate based on statistical fluctuations proportional to the square-root of the number of collisions studied. The relatively complicated dependence of the results on field strength suggests

that the external field method is advantageous only if it is desired to know the nonlinear conductivity. The linear conductivity can as easily be found using the Green-Kubo technique, which has the added advantage of providing the other transport coefficients and their frequency dependence simultaneously.

The nonlinear conductivity is interesting. Both the 4-sphere and 32-sphere results are approximately linear in $\lambda^{1/2}$ for larger fields. This dependence can be thought of as arising from a diffusion process or, alternatively, from a scattering process. In the former case the diffusion equation suggests a fall-off in correlation as time$^{3/2}$ in three dimensions, leading to a frequency dependence or field dependence of order $\omega^{1/2}$ or $\lambda^{1/2}$. Alternatively, from the standpoint of scattering of phonons, the Debye-Waller scattering, proportional to the average value of ω^{-2}, and combined with a density of states proportional to ω^2, leads also to a square-root dependence.

The nonlinear conductivities found here, increasing with field in the solid and dense fluid phases, could be extended and made more precise were there data available from other simulations for comparison. There appear to be no difficulties in extending the non-equilibrium techniques to hard spheres. The hard-sphere model is particularly suited to shock wave simulation, the area in which nonlinear effects are most easily generated and studied.

ACKNOWLEDGMENTS

W.G. Hoover thanks the Universities of California and Vienna, as well as the Lawrence Livermore National Laboratory, for support during a sabbatical leave which led to this work. Work at the Lawrence Livermore National Laboratory was carried out under Contract No. W-7405-ENG-48. Work at the University of Vienna was carried out with the active encouragement of Prof. Dr. Peter Weinzierl. Mag. Karlsreiter provided invaluable help with the computer system at the University of Vienna.

REFERENCES

1. S. Chapman and T.G. Cowling, The Mathematical Theory of Non-Uniform Gases, Cambridge University Press (1970).

2. B.J. Alder and T.E. Wainwright, "Studies in Molecular Dynamics: Behavior of a Small Number of Elastic Spheres", Journal of Chemical Physics 33, 1439 (1960).,

3. B.J. Alder, D.M. Gass and T.E. Wainwright, "Studies in Molecular Dynamics: Transport Coefficients for Hard Spheres", Journal of Chemical Physics 53, 3813 (1970).

4. W.G. Hoover and B.J. Alder, "Studies in Molecular Dynamics, The Pressure, Collision Rate, and Their Number-Dependence for Hard Disks", Journal of Chemical Physics 46, 686 (1967).

5. W.G. Hoover and F.H. Ree, "Melting Transition and Communal Entropy for Hard Spheres", Journal of Chemical Physics 49, 3609 (1968).

6. H.S. Kang, C.S. Lee, T. Ree, and F.H. Ree, "A Perturbation Theory of Classical Equilibrium Fluids", Journal of Chemical Physics 84, 4547 (1986).

7. W.G. Hoover, "Computer Simulation of Many-Body Dynamics", Physics Today 44 (January 1984).

8. D.J. Evans and W.G. Hoover, "Flows Far From Equilibrium via Molecular Dynamics", Annual Review of Fluid Mechanics 10, 243 (1986).

9. D.J. Evans, "Homogeneous Nonequilibrium Molecular Dynamics Algorithm for Thermal Conductivity - Application of Non-Canonical Linear Response Theory", Physics Letters 91A, 457 (1982).

10. M. Dixon and M.J. Gillan, "Calculation of Thermal Conductivities by Perturbed Molecular Dynamics Simulation", Journal of Physics C16, 869 (1983).

11. W.G. Hoover, B. Moran, and J. Haile, "Homogeneous Periodic Heat Flow via Nonequilibrium Molecular Dynamics", Journal of Statistical Physics 37, 109 (1983).

12. W.G. Hoover, G. Cicotti, G. Paolini, and C. Massobrio, "Lennard-Jones Triple-Point Conductivity via Weak External Fields. Additional Results", Physical Review A 32, 3765 (1986).

13. W.G. Hoover and K.W. Kratky, "Heat Conductivity of Three Periodic Hard Disks via Nonequilibrium Molecular Dynamics", Journal of Statistical Physics 42, 1103 (1986).

14. W.G. Hoover, "Nonlinear Conductivity and Entropy in the Two-Body Boltzmann Gas", Journal of Statistical Physics 42, 587 (1986).

15. K.W. Kratky, "Fluctuation of Thermodynamic Parameters in Different Ensembles", Physical Review A 31, 945 (1985).

16. R. Grover, W.G. Hoover, and B. Moran, "Corresponding States for Thermal Conductivities via Nonequilibrium Moleculear Dynamics", Journal of Chemical Physics 83, 1255 (1985).

TABLE I. Number of computer runs and of collisions as a function of λ. Each run started from a FCC lattice with different random initial velocities. The first 500 collisions were used for equilibration, the consecutive 2500 for calculation.

$\lambda^{1/2}$	No.(runs)	No.(collisions)
0.0 to 0.2	24	60 000
0.3	20	50 000
0.4	16	40 000
0.5	12	30 000
0.6 to 2.0	8	20 000

TABLE II. Quantities calculated in the computer runs , $m = \sigma = kT = 1$.

$\bar{t}^{str}$	Average time of streaming motion (between collisions), inverse of the collision rate
Z_E	Compressibility factor $P_E V/(NkT)$ for the isoenergetic case, calculated from pressure t
$\bar{Q}_{x,E}$	Average heat flux in the x-direction (isoenergetic case)
$\varkappa_E/k$	Total heat conductivity over k (isoenergetic case)
$\varkappa^{str}/k$	Contribution of streaming motion to the heat conductivity
$\left(\frac{Z_K - 1}{Z_E - 1}\right)$	Ratio (isokinetic/isoenergetic) for the collisional part of Z
$\left(\frac{\varkappa_K^{coll}}{\varkappa_E^{coll}}\right)$	Ratio (isokinetic/isoenergetic) for the collisional part of $\varkappa$

The numbers in parentheses denote the uncertainty of the last digit(s) of the results displayed in Tables III to VIII.

TABLE III. Results of nonequilibrium molecular dynamics for hard spheres. N=4, V/V_o=1.25. The calculated quantities are explained in Table II.

$\lambda^{1/2}$	$10^2\bar{t}^{str}$	z_E	$\bar{Q}_{x,E}$	$\varkappa_E/k$	$\varkappa^{str}/k$	$\left(\frac{z_K-1}{z_E-1}\right)$	$\left(\frac{\varkappa_K^{coll}}{\varkappa_E^{coll}}\right)$
0.0	1.242(3)	14.36(0)	-----	-----	-----	1.126	-----
0.1	1.242(2)	14.36(0)	-----	-----	-----	1.124	-----
0.2	1.243(3)	14.36(0)	0.17(6)	4.29(144)	0.24(15)	1.126	1.379
0.3	1.243(3)	14.36(0)	0.60(7)	6.65(79)	0.56(8)	1.125	1.461
0.4	1.244(2)	14.37(0)	0.77(9)	4.80(58)	0.38(5)	1.125	1.484
0.5	1.242(4)	14.37(0)	1.25(7)	5.01(28)	0.38(2)	1.126	1.408
0.6	1.242(4)	14.37(1)	1.89(8)	5.25(23)	0.38(2)	1.124	1.396
0.7	1.236(3)	14.39(1)	2.81(11)	5.73(23)	0.43(1)	1.121	1.398
0.8	1.233(4)	14.40(1)	3.28(16)	5.13(25)	0.38(2)	1.122	1.406
0.9	1.234(6)	14.40(2)	4.14(14)	5.12(17)	0.37(1)	1.120	1.392
1.0	1.228(3)	14.41(2)	5.10(14)	5.10(14)	0.37(1)	1.117	1.375
1.1	1.229(4)	14.45(1)	5.71(10)	4.72(12)	0.33(1)	1.117	1.363
1.2	1.221(5)	14.43(2)	6.67(21)	4.63(14)	0.32(1)	1.115	1.356
1.3	1.217(2)	14.39(2)	7.38(7)	4.37(4)	0.29(1)	1.112	1.344
1.4	1.231(5)	14.32(2)	8.32(13)	4.25(7)	0.27(1)	1.112	1.334
1.5	1.226(5)	14.29(4)	8.73(13)	3.88(6)	0.24(1)	1.110	1.321
1.6	1.245(5)	14.18(2)	9.53(7)	3.72(3)	0.22(0)	1.110	1.319
1.7	1.243(7)	14.13(3)	10.16(14)	3.52(5)	0.20(0)	1.107	1.307
1.8	1.263(6)	13.88(3)	10.53(8)	3.25(2)	0.18(0)	1.105	1.295
1.9	1.265(4)	13.81(4)	10.87(9)	3.01(2)	0.15(0)	1.103	1.280
2.0	1.287(3)	13.66(4)	11.30(6)	2.83(1)	0.14(0)	1.103	1.274

TABLE IV. As Table III, except for N=32, V/V_o=1.25.

$\lambda^{1/2}$	$10^2\bar{t}^{str}$	z_E	$\bar{Q}_{x,E}$	$\varkappa_E/k$	$\varkappa^{str}/k$	$(\frac{z_K-1}{z_E-1})$	$(\frac{\varkappa_K^{coll}}{\varkappa_E^{coll}})$
0.0	0.137(0)	14.67(1)	-----	-----	-----	1.011	-----
0.1	0.137(0)	14.68(1)	-----	-----	-----	1.011	-----
0.2	0.137(0)	14.67(1)	0.9(1)	21.5(32)	1.34(25)	1.011	1.033
0.3	0.137(0)	14.68(1)	1.6(1)	17.6(15)	1.11(12)	1.011	1.034
0.4	0.138(1)	14.65(1)	2.7(1)	17.0(7)	1.10(5)	1.011	1.035
0.5	0.137(0)	14.66(1)	4.0(2)	15.9(7)	1.04(5)	1.011	1.037
0.6	0.138(1)	14.63(1)	6.1(2)	16.8(6)	1.10(4)	1.011	1.039
0.7	0.139(1)	14.56(2)	8.4(3)	17.2(5)	1.15(5)	1.012	1.041
0.8	0.139(1)	14.56(3)	10.5(3)	16.5(5)	1.11(4)	1.012	1.040
0.9	0.141(1)	14.51(3)	14.3(5)	17.6(7)	1.14(15)	1.013	1.048
1.0	0.142(1)	14.44(5)	18.2(5)	18.2(5)	1.32(5)	1.014	1.054
1.1	0.144(1)	14.47(5)	23.3(5)	19.2(4)	1.43(4)	1.015	1.059
1.2	0.149(1)	14.31(5)	28.2(6)	19.6(4)	1.51(4)	1.017	1.066
1.3	0.155(1)	14.13(7)	33.3(7)	19.7(4)	1.57(5)	1.019	1.077
1.4	0.165(1)	13.74(7)	38.7(11)	19.7(6)	1.63(7)	1.022	1.086
1.5	0.174(1)	13.53(4)	43.1(7)	19.2(3)	1.61(3)	1.024	1.091
1.6	0.182(2)	13.25(10)	46.0(10)	18.0(4)	1.54(3)	1.025	1.091
1.7	0.204(1)	12.79(8)	53.3(9)	18.4(3)	1.59(2)	1.030	1.103
1.8	0.212(3)	12.41(10)	54.0(9)	16.7(3)	1.47(3)	1.030	1.101
1.9	0.230(3)	12.13(7)	58.7(7)	16.3(2)	1.46(1)	1.032	1.105
2.0	0.256(3)	11.72(6)	62.3(6)	15.6(2)	1.42(1)	1.035	1.109

Table V. As Table III, except for N=4, V/V_o=1.80.

$\lambda^{1/2}$	$10^2 \bar{t}^{str}$	z_E	$\bar{Q}_{x,E}$	$\varkappa_E/k$	$\varkappa^{str}/k$	$(\frac{z_K-1}{z_E-1})$	$(\frac{\varkappa_K^{coll}}{\varkappa_E^{coll}})$
0.0	3.12(1)	6.30(1)	-----	-----	-----	1.125	-----
0.1	3.12(1)	6.32(1)	-----	-----	-----	1.124	-----
0.2	3.13(1)	6.31(1)	0.06(2)	1.53(48)	0.32(8)	1.125	1.480
0.3	3.12(1)	6.31(1)	0.19(2)	2.15(25)	0.34(4)	1.124	1.398
0.4	3.13(1)	6.32(1)	0.36(3)	2.26(19)	0.37(3)	1.126	1.432
0.5	3.13(2)	6.31(1)	0.62(3)	2.48(11)	0.41(2)	1.123	1.409
0.6	3.13(2)	6.31(1)	0.80(4)	2.22(10)	0.34(2)	1.126	1.388
0.7	3.11(1)	6.33(1)	1.10(5)	2.24(9)	0.36(1)	1.124	1.391
0.8	3.10(1)	6.34(2)	1.32(4)	2.06(6)	0.32(1)	1.122	1.379
0.9	3.12(1)	6.34(1)	1.65(5)	2.03(6)	0.32(1)	1.123	1.384
1.0	3.11(1)	6.36(2)	1.92(3)	1.92(3)	0.30(1)	1.121	1.375
1.1	3.12(2)	6.36(3)	2.33(4)	1.93(3)	0.30(1)	1.122	1.379
1.2	3.13(2)	6.34(2)	2.63(2)	1.83(1)	0.28(0)	1.121	1.369
1.3	3.14(2)	6.35(1)	2.98(4)	1.76(2)	0.27(0)	1.122	1.370
1.4	3.19(1)	6.29(2)	3.22(3)	1.64(2)	0.25(0)	1.121	1.358
1.5	3.16(2)	6.35(3)	3.57(5)	1.59(2)	0.23(0)	1.123	1.360
1.6	3.21(2)	6.28(5)	3.76(5)	1.47(2)	0.21(0)	1.124	1.355
1.7	3.27(2)	6.20(4)	3.98(5)	1.38(2)	0.20(0)	1.125	1.354
1.8	3.32(2)	6.18(4)	4.25(4)	1.31(1)	0.19(0)	1.129	1.356
1.9	3.36(2)	6.18(4)	4.38(3)	1.21(1)	0.17(0)	1.132	1.358

TABLE VI. As Table III, except for N=32, V/V_o=1.80.

$\lambda^{1/2}$	$10^2\bar{t}^{str}$	z_E	$\bar{Q}_{x,E}$	$\varkappa_E/k$	$\varkappa^{str}/k$	$\left(\frac{z_K-1}{z_E-1}\right)$	$\left(\frac{\varkappa_K^{coll}}{\varkappa_E^{coll}}\right)$
0.0	0.285(1)	7.58(2)	-----	-----	-----	1.011	-----
0.1	0.284(1)	7.57(3)	-----	-----	-----	1.011	-----
0.2	0.282(1)	7.62(3)	0.3(1)	7.3(13)	0.83(21)	1.011	1.039
0.3	0.282(1)	7.62(3)	0.6(0)	6.2(3)	0.84(6)	1.011	1.038
0.4	0.285(1)	7.58(3)	1.1(1)	7.0(4)	0.89(7)	1.011	1.038
0.5	0.283(2)	7.62(5)	1.7(1)	6.8(3)	0.78(8)	1.011	1.037
0.6	0.285(2)	7.64(3)	2.6(1)	7.3(3)	0.87(5)	1.012	1.043
0.7	0.288(3)	7.59(6)	3.6(2)	7.4(4)	0.89(3)	1.012	1.042
0.8	0.294(2)	7.50(5)	5.3(2)	8.3(4)	1.10(6)	1.013	1.055
0.9	0.308(2)	7.29(6)	6.7(3)	8.3(4)	1.22(7)	1.014	1.062
1.0	0.332(3)	7.13(5)	9.8(3)	9.8(3)	1.48(5)	1.019	1.078
1.1	0.354(2)	7.05(7)	12.9(4)	10.7(3)	1.64(4)	1.022	1.087
1.2	0.382(6)	6.86(7)	15.1(5)	10.5(3)	1.73(10)	1.027	1.104
1.3	0.428(4)	6.68(5)	18.5(6)	10.9(4)	1.83(5)	1.032	1.118
1.4	0.458(6)	6.54(7)	20.2(3)	10.3(2)	1.77(5)	1.035	1.121
1.5	0.520(8)	6.37(8)	23.6(5)	10.5(2)	1.81(3)	1.041	1.136
1.6	0.565(7)	6.21(8)	24.5(5)	9.6(2)	1.73(4)	1.044	1.135
1.7	0.611(7)	5.99(6)	25.6(4)	8.9(1)	1.62(1)	1.045	1.134
1.8	0.677(7)	5.80(8)	26.9(5)	8.3(2)	1.56(2)	1.049	1.141
1.9	0.710(11)	5.70(6)	27.4(5)	7.6(1)	1.44(2)	1.049	1.137
2.0	0.734(12)	5.73(9)	29.2(3)	7.3(1)	1.37(2)	1.050	1.136

TABLE VII. As Table III, except for N=4, V/V_o=3.00.

$\lambda^{1/2}$	$10^2\bar{t}^{str}$	z_E	$\bar{Q}_{x,E}$	$\varkappa_E/k$	$\varkappa^{str}/k$	$(\frac{z_K-1}{z_E-1})$	$(\frac{\varkappa_K^{coll}}{\varkappa_E^{coll}})$
0.0	5.88(3)	3.82(1)	-----	-----	-----	1.125	-----
0.1	5.91(3)	3.80(2)	-----	-----	-----	1.124	-----
0.2	5.86(3)	3.83(1)	0.05(1)	1.33(28)	0.29(7)	1.125	1.378
0.3	5.87(3)	3.82(2)	0.11(1)	1.26(14)	0.27(4)	1.126	1.355
0.4	5.92(3)	3.81(2)	0.19(1)	1.21(6)	0.29(3)	1.125	1.398
0.5	5.88(3)	3.83(2)	0.30(1)	1.20(5)	0.30(2)	1.124	1.366
0.6	5.85(6)	3.82(3)	0.42(1)	1.15(4)	0.28(1)	1.123	1.362
0.7	5.91(6)	3.82(3)	0.56(2)	1.13(4)	0.28(1)	1.125	1.374
0.8	6.10(4)	3.73(2)	0.70(3)	1.10(4)	0.29(1)	1.122	1.342
0.9	6.08(5)	3.76(2)	0.81(2)	1.00(2)	0.26(1)	1.125	1.359
1.0	6.09(3)	3.74(1)	0.91(2)	0.91(2)	0.23(0)	1.124	1.340
1.1	6.19(6)	3.71(2)	1.06(2)	0.87(1)	0.22(1)	1.122	1.327
1.2	6.24(3)	3.69(2)	1.16(1)	0.80(1)	0.22(1)	1.123	1.330
1.3	6.33(4)	3.65(2)	1.28(1)	0.76(1)	0.21(0)	1.124	1.334
1.4	6.61(4)	3.53(2)	1.33(2)	0.68(1)	0.20(0)	1.122	1.334
1.5	6.69(3)	3.52(2)	1.40(1)	0.62(1)	0.19(0)	1.123	1.330
1.6	6.94(3)	3.42(2)	1.47(2)	0.58(1)	0.18(0)	1.121	1.325
1.7	6.78(22)	3.38(2)	1.55(2)	0.54(1)	0.17(0)	1.120	1.311
1.8	7.27(6)	3.32(2)	1.61(2)	0.50(1)	0.16(0)	1.113	1.308

TABLE VIII. The results of Tables III to VII, extrapolated to equilibrium.

N	V/V_o	$10^2\bar{t}^{str}$	z_E	$\varkappa_E/k$	$\varkappa^{str}/k$
4	1.25	1.243(0)	14.362(2)	5.18(18)	0.39(2)
32	1.25	0.137(0)	14.666(5)	16.74(36)	1.09(2)
4	1.80	3.124(2)	6.312(2)	2.30(8)	0.37(2)
32	1.80	0.284(1)	7.603(10)	6.79(21)	0.85(2)
4	3.00	5.885(9)	3.820(5)	1.18(2)	0.28(0)